

Spin-related physics
in
integer quantum Hall system

Ming-Che Chang
Department of physics
Taiwan Normal University

Outline

Multi-component quantum Hall system

spin, layer, or valley (for Si) degrees of freedom

Spin: Quantum Hall ferro-magnet

Collective excitation and quasi-particle in QHFM

Spin wave, skyrmion

Layer: $\nu=1$ Bilayer system as a QH pseudo-FM

Collective excitation and quasi-particle in QHpFM

Pseudo-spin wave, meron

Josephson-like effect in bilayer system

$\nu=2$ Three different quantum phases

Ferromagnet, canted antiferromagnet, and spin-singlet

The effect of in-plane magnetic field

Layout of a quantum Hall system

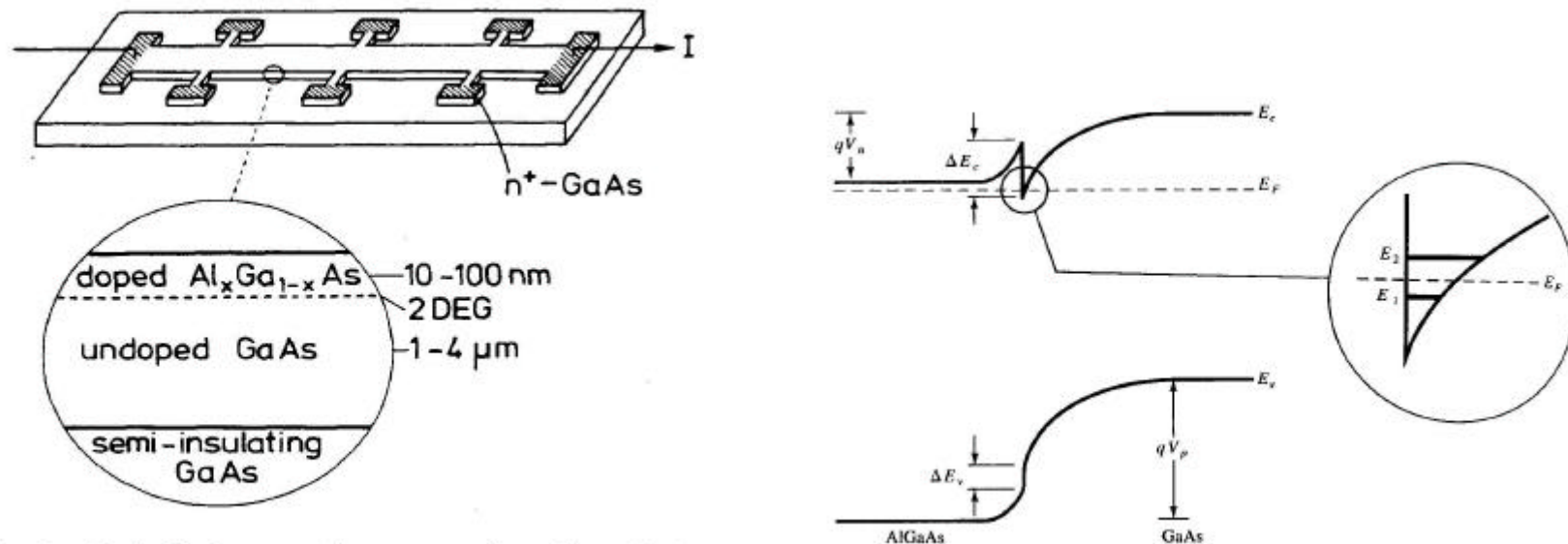
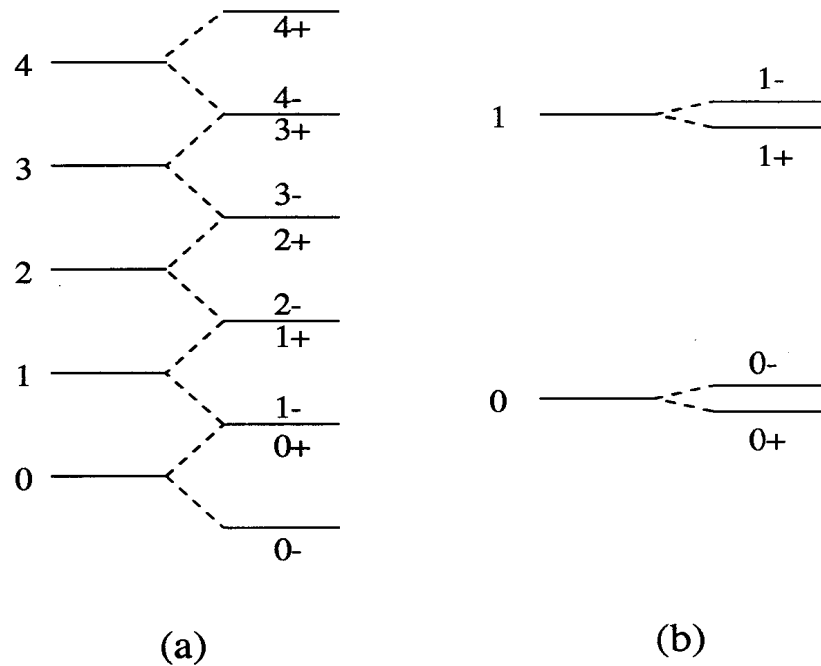


FIG. 3. Typical shape and cross section of a GaAs-Al_xGa_{1-x}As heterostructure used for Hall-effect measurements.

Landau levels



Strong magnetic field (> 1 T)

Low temperature (< 4 K)

Figure 1.22: (a) Landau energy levels for an electron in free space. Numbers label the Landau levels and $+(-)$ refers to spin up (down). Since the g factor is 2, the Zeeman splitting is exactly equal to the Landau level spacing, $\hbar\omega_c$ and there are extra degeneracies as indicated. (b) Same for an electron in GaAs. Because the effective mass is small and $g \approx -0.4$, the degeneracy is strongly lifted and the spin assignments are reversed.

Some important parameters

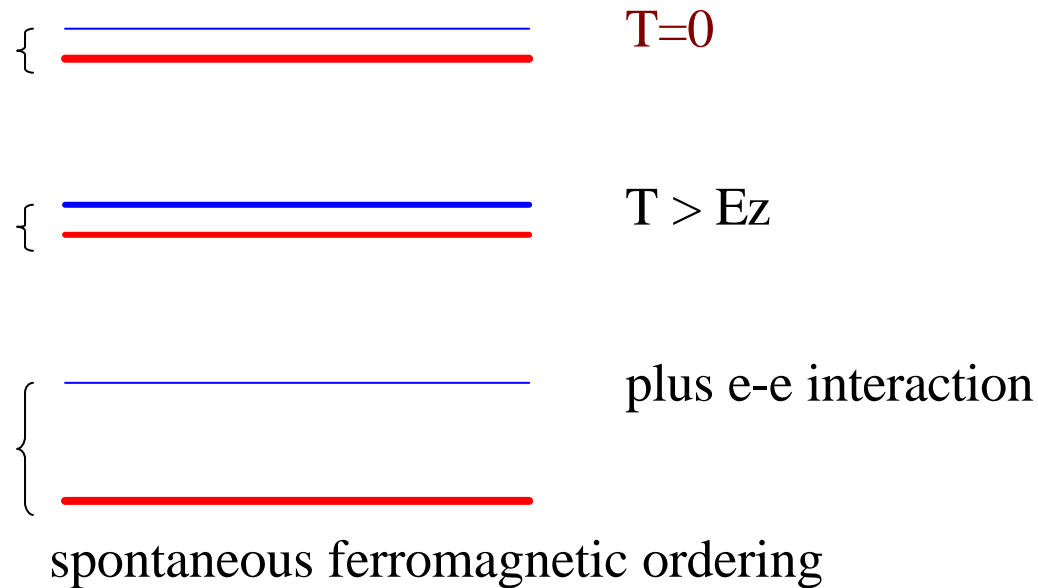
Typical length scale: magnetic length $\ell \equiv \sqrt{\hbar/eB} \approx 128 \text{ \AA}$ at 4 T

Material dep.	{	Dielectric constant: 12.8	$e^2/\epsilon l \approx 100 \text{ K}$ at 4 T
		Effective mass: 0.068 m_e	$\hbar\omega_c \approx 80 \text{ K}$ at 4 T
		0.38 m_e (LH), 0.6 m_e (HH)	
GaAs/AlGaAs	{	g factor: -0.44, spin-orbit effect	
		$g\mu_B B \approx 1 \text{ K}$ at 4 T	

Sample dep.	{	Landau level degeneracy: $D_{LL} = B \times (\text{sample area}) / \Phi_0$
		mobility ($10^4 - 10^6 \text{ cm}^2/\text{Vs}$), electron density ($10^{11} / \text{cm}^2$)

Physics in the Lowest Landau Level (LLL): integer case

Filling factor $\nu = 1$



single spin flip costs $\Sigma = (\pi/2)^{1/2} e^2/\epsilon l = 125 \text{ K at } 4 \text{ T}$

QHFM: an itinerant ferromagnet with quantized Hall resistances

The wave function is simply the $m=1$ Laughlin wave function

→ the world's best understood ferromagnet

Manybody effect on the “Zeeman splitting”

$$v_{\uparrow} = 1: \quad g^* \mu_B \mathbf{B} = g \mu_B \mathbf{B} + \Sigma, \quad \Sigma = (\pi/2)^{1/2} e^2 / \epsilon l$$

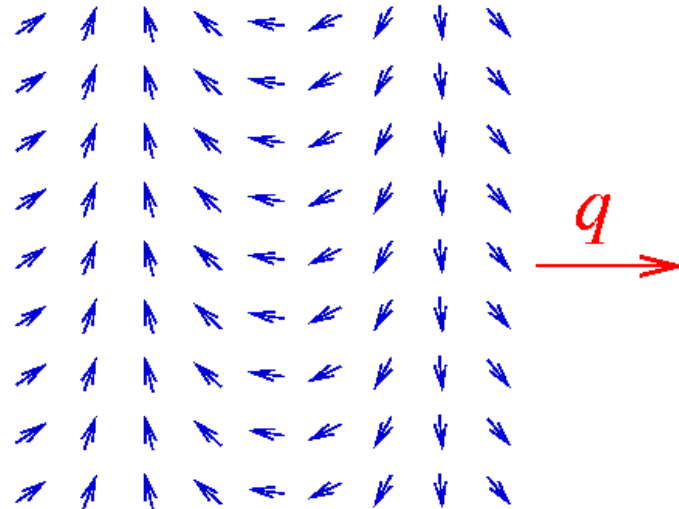
$$v_{\uparrow} < 1: \quad g^* \mu_B \mathbf{B} = g \mu_B \mathbf{B} + \Sigma_{\times} [n_{\uparrow}(g^*) - n_{\downarrow}(g^*)],$$

need to be solved self-consistently, Ando+Uemura 1974

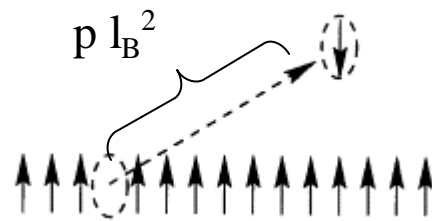
→ oscillatory behavior

Spin-related elementary excitations in QHFM

Spin wave



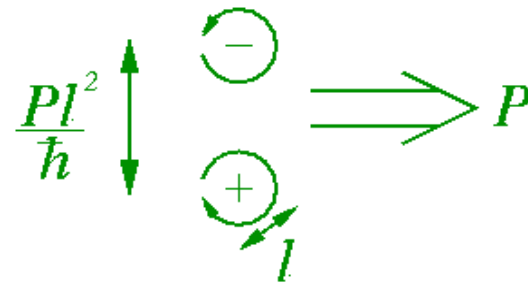
coherent superposition of e-h pairs



LLL projection

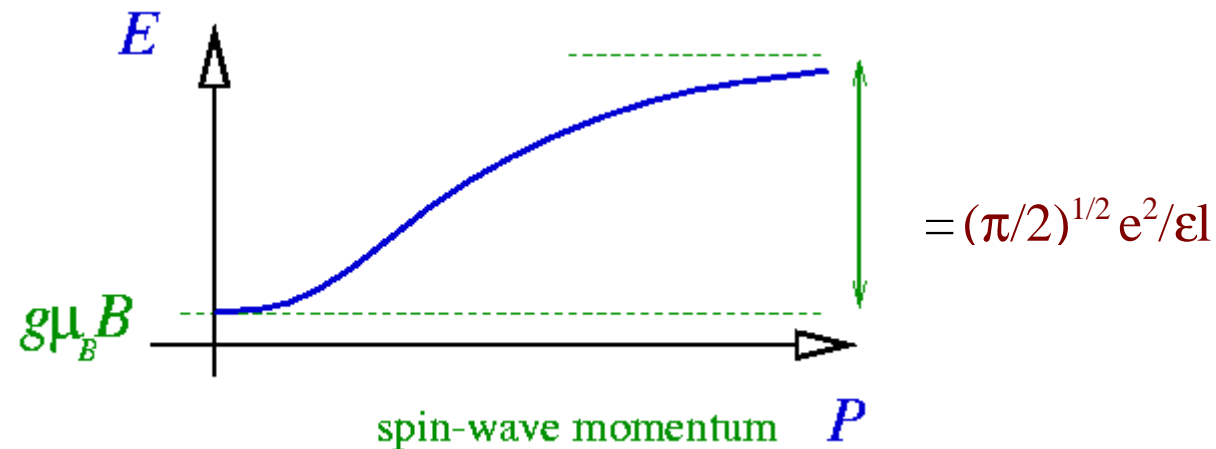
$$|\psi_{\mathbf{p}}\rangle = \sum_i e^{i\mathbf{p}\cdot\mathbf{r}_i} c_{i\downarrow}^\dagger c_{i\uparrow} |\psi_0\rangle$$

Semiclassical Picture:



Dispersion Relation ($\nu = 1$)

[Lerner & Lozovik, 1980]



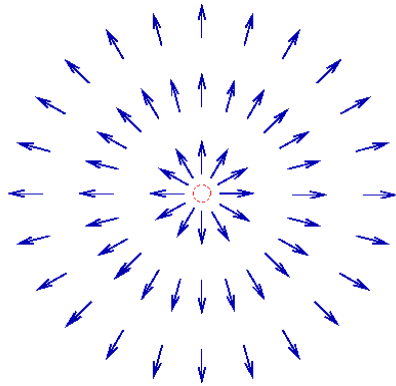
$Pl/\hbar \rightarrow \infty \implies$ quasielectron/quasihole pair.

Are these the lowest-energy charged excitations?

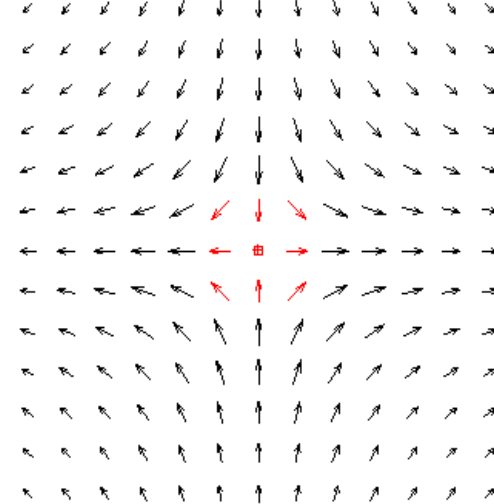
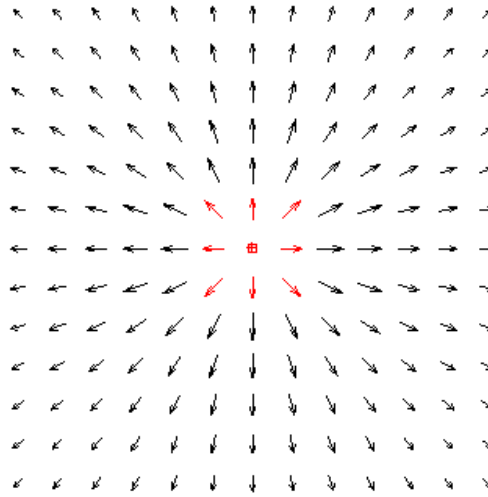
skyrmion – charged spin-texture excitation [Sondhi et al, 1993] –

different forms of spin texture in 2D:

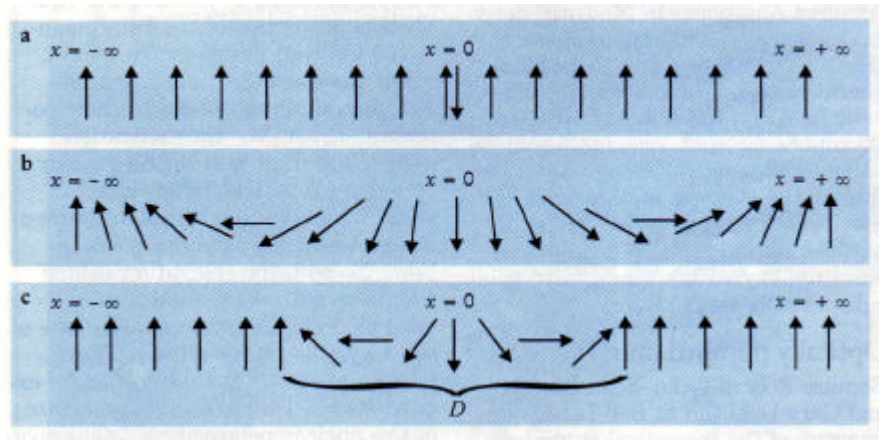
easy plane, vortex



easy axis, antiskyrmion / skyrmion



Formation of a skyrmion



Noninteracting

Plus e-e interaction

Plus Zeeman energy

$g \ll 1$: larger extent of distorted spins is better

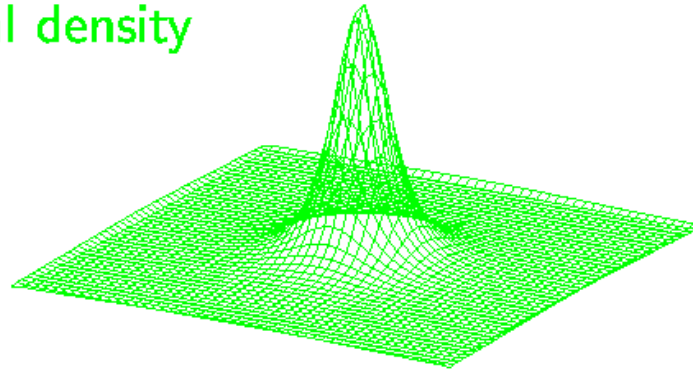
→ rapid depolarization by adding one skyrmion

$g \gg 1$: only one spin is flipped

The skyrmion is charged

Spin texture determines charge density profile

Topological density



Topological charge of spin texture

$$Q_{\text{top}} \equiv \frac{1}{8\pi} \int d^2r \epsilon^{\alpha\beta} \vec{m} \cdot \partial_\alpha \vec{m} \times \partial_\beta \vec{m} = \text{integer}$$

Q_{top} is the wrapping number of the $S^2(\mathbf{r}) \rightarrow S^2(\mathbf{m})$ mapping
stable against smooth continuous distortion of $\mathbf{m}(\mathbf{r})$

Electric charge $Q = v e Q_{\text{top}}$

Barrett et al, 1995.

NMR

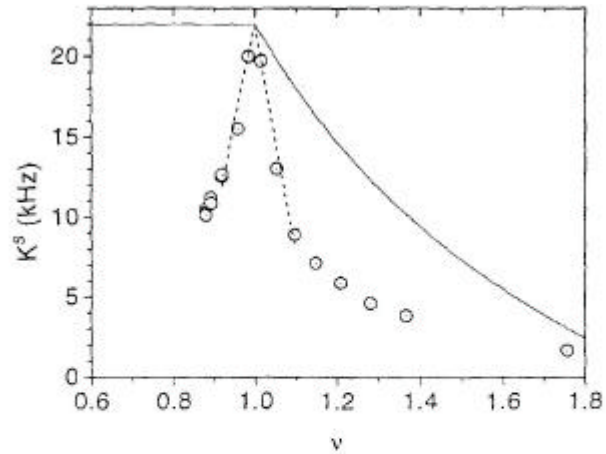


FIG. 3. Dependence of K^s on filling factor ν for $B = 7.05$ T (open circles) at 1.55 K. As explained in the text, both fits are given by Eq. (1), but the solid line has $\mathcal{A} = \mathcal{S} = 1$ (noninteracting electrons), while the dashed line has $\mathcal{A} = \mathcal{S} = 3.6$ (finite-size Skyrmions).

Schmeller et al, 1995.

magnetotransport

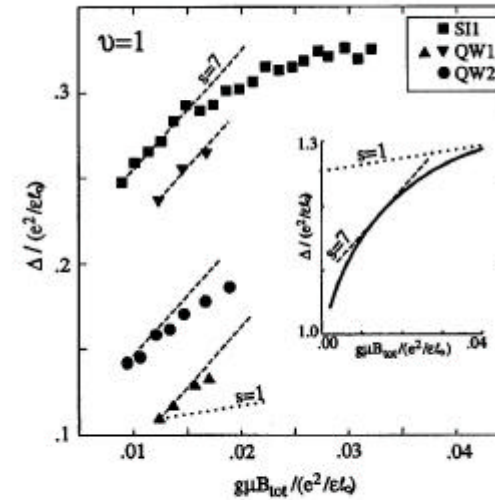


FIG. 2. Results of tilted-field experiments on the $\nu = 1$ QHE. The energy gaps Δ at fixed B_{\perp} are plotted vs the Zeeman energy $g\mu_B B_{\text{tot}}$, both in units of $e^2/\epsilon\epsilon_0$. Each data set starts with $\theta = 0$ and $B_{\text{tot}} = B_{\perp}$ at the lower left. On the quantum well samples we use gate electrodes to tune the electron densities [11]. From top to bottom the samples had electron densities $0.6, 1.0, 0.6,$ and $1.0 \times 10^{11} \text{ cm}^{-2}$ and mobilities $3.4, 0.52, 0.18,$ and $0.16 \times 10^6 \text{ cm}^2/\text{Vs}$, respectively. For comparison we include lines with $\partial\Delta/\partial(g\mu_B B_{\text{tot}}) = s = 7$ (dashed) and 1 (dotted). The inset shows a Hartree-Fock result of Skyrmion theory (full line) [514].

Maude et al, 1996
magnetotransport

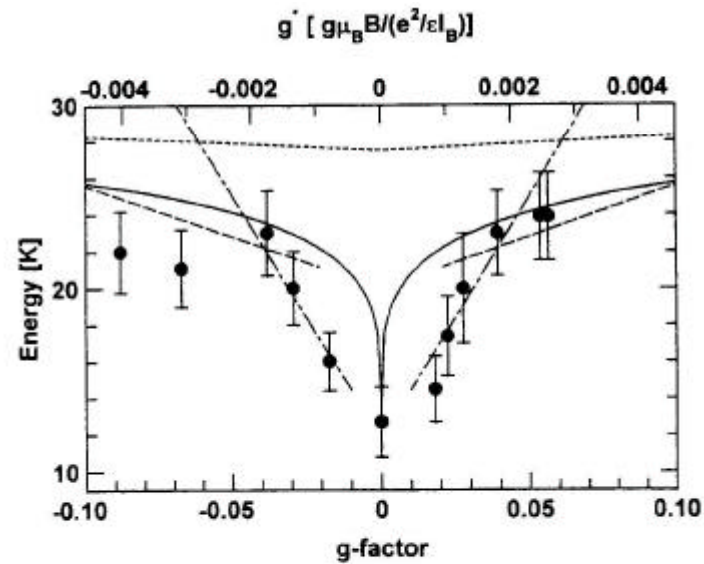
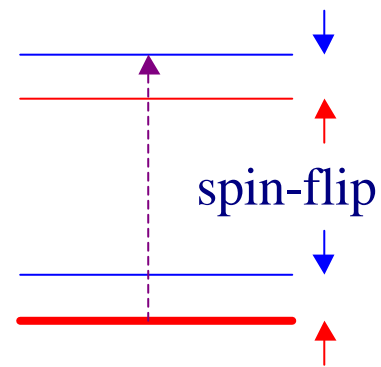
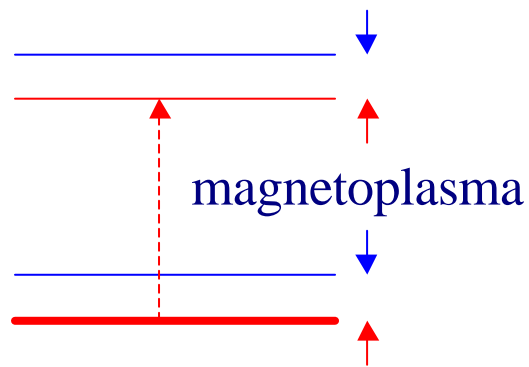


FIG. 3. The measured energy gap at filling factor $\nu = 1$ as a function of the bare g factor (bottom axis) and as a function of g^* , the ratio of the Zeeman and Coulomb energies (top axis). The solid line is the expected gap for a Skyrmion-type excitation [7], while the short-dashed line indicates the expected variation for the "bare" Zeeman dependence $E_B + s|g|\mu_B B$ (with $s = 1$ as predicted by the spin-wave dispersion model). Lines with slopes corresponding to $s = 7$ spin flips (long-dashed line) and $s = 33$ spin flips (long-short-dashed line) are shown for comparison.

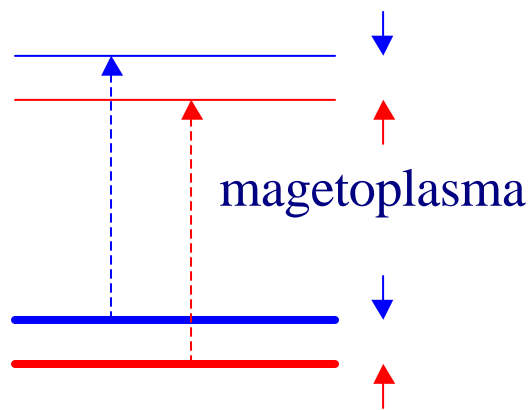
Inter-Landau level excitations

Different ways to lift an electron from $n=0$ to $n=1$:

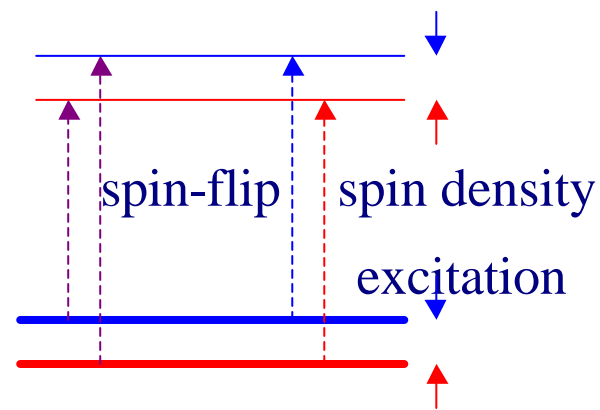
$\nu = 1$



$\nu = 2$



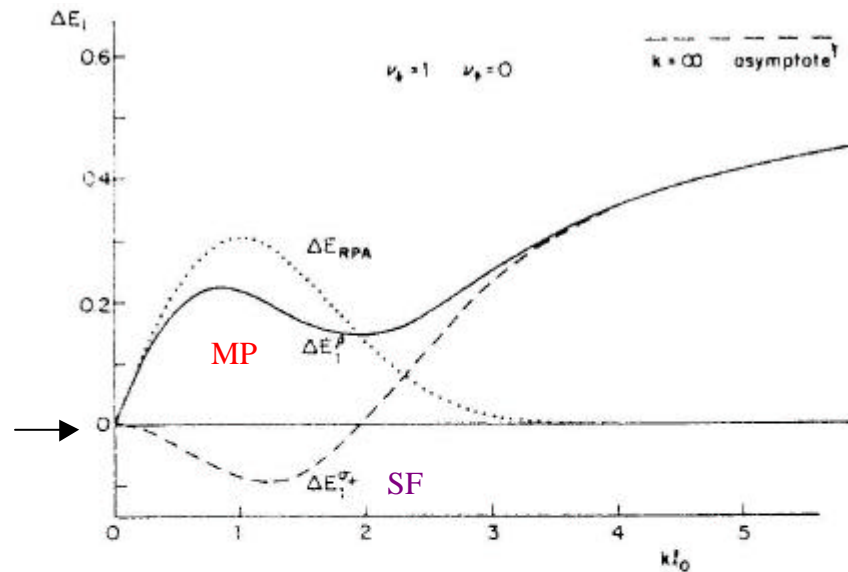
(singlet exciton)



(triplet exciton)

$\nu = 1$ [Kallin + Halperin, 1984]

Kohn's theorem →



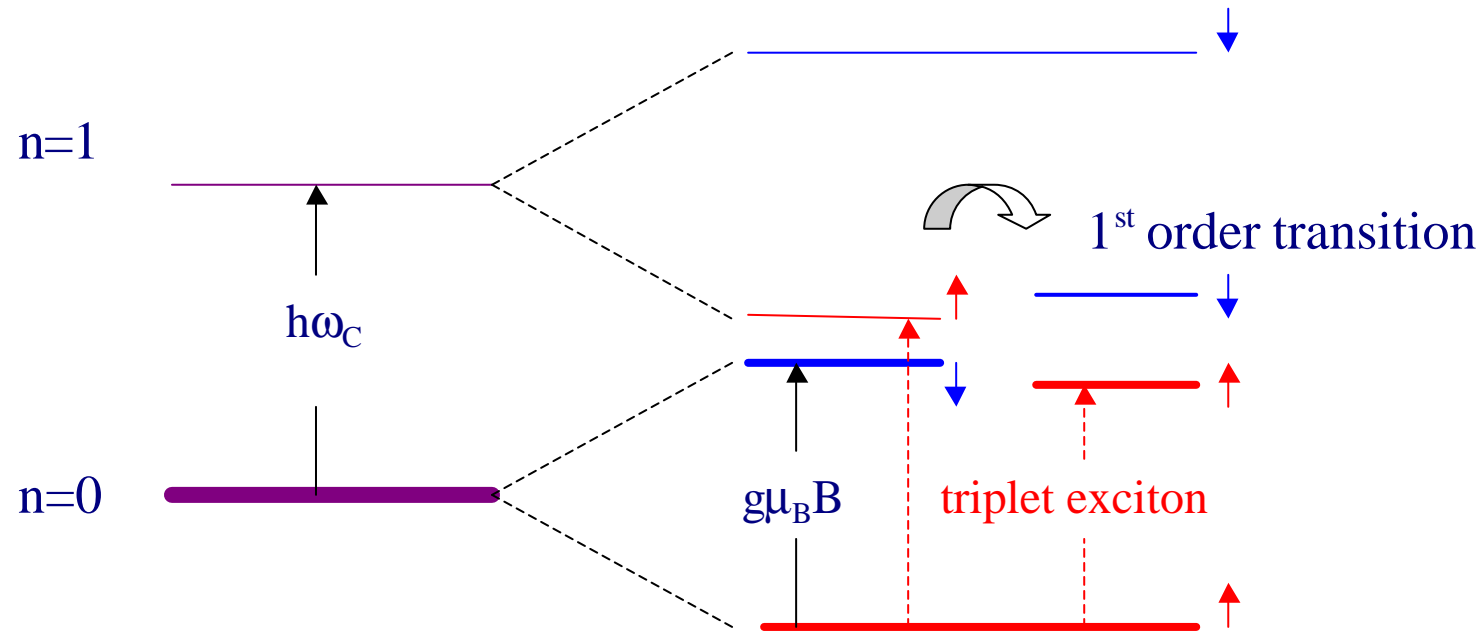
$(\pi/2)^{1/2} e^2/\epsilon l$

FIG. 3. Energy shifts for a spin-polarized sample with only the lowest Landau level filled, $\nu_{\uparrow}=1$ and $\nu_{\downarrow}=0$, and $m=1$ are shown. The energy scale is in units of $e^2/\epsilon l_0$. The solid curve denotes $\Delta E_1^{\rho} = E_1^{\rho}(k) - \omega_c$, where $\omega = E_1^{\rho}(k)$ is the pole in the density response function χ_{ρ} . The same pole appears in χ_{σ_z} also. The dashed curve denotes $\Delta E_1^{\sigma+} = E_1^{\sigma+} - \omega_c - |g\mu_B B|$, where $\omega = E_1^{\sigma+}$ is the pole in the spin-response function $\chi_{\sigma+}$. The RPA energy shift, $E_{RPA} - \omega_c$, is denoted by the dotted curve.

$$\nu = 2$$

spin-polarization instability in a tilted magnetic field

[Giuliani + Quinn, 1985]



paramagnetic \rightarrow ferromagnetic phase transition

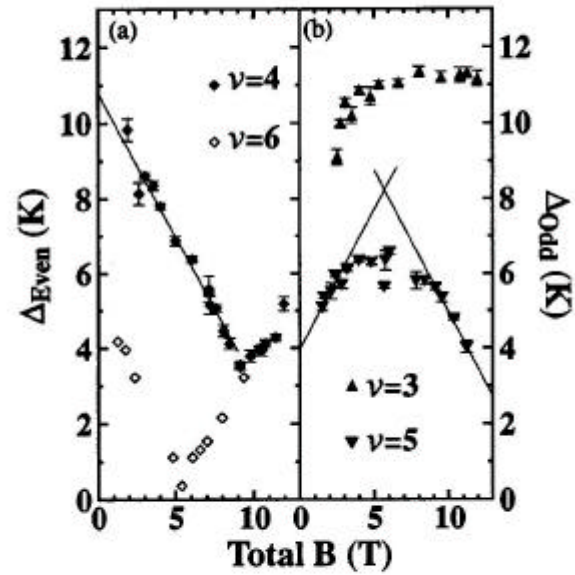
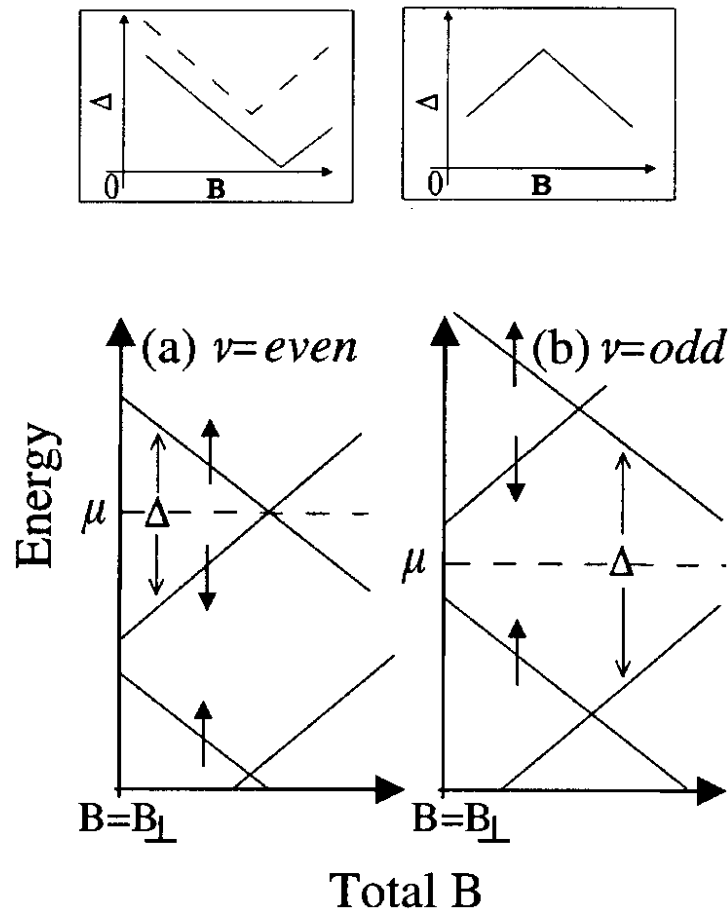
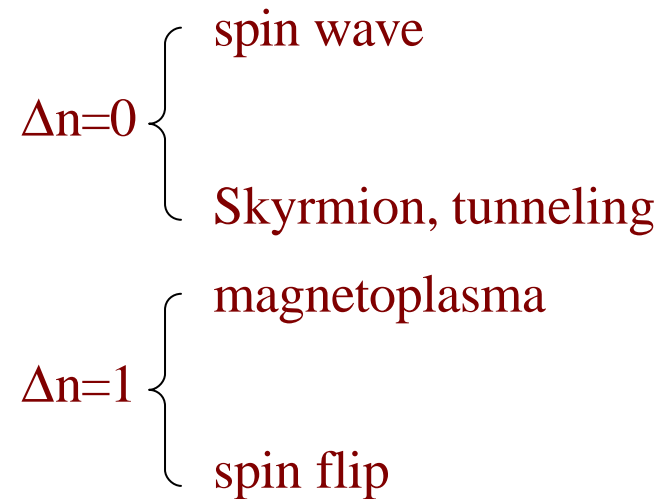


FIG. 3. (a) Filled symbols show the energy gaps measured at $\nu = 4$ as a function of the total magnetic field applied to the sample. Δ_4 drops linearly to a gap of 3.5 ± 0.1 K at its turning point at 9.13 T. The solid line is a fit to the Δ_4 data below 7.2 T with the slope corresponding to a g factor of 1.1. Open symbols show similar data for $\nu = 6$. (b) The energy gaps Δ_3 and Δ_5 at odd filling factors. Δ_5 exhibits distinct curvature near to its turning point at 5.7 T. The solid lines have the same gradients as the line in (a), and demonstrate that away from 6 T the data are consistent with the g factor measured at $\nu = 4$.

Summary

$\nu = 1$ Quantum Hall ferromagnet

spin-related excitations



$\nu = 2$ Quantum Hall paramagnet

Giuliani-Quinn instability, PM \rightarrow FM transition

bilayer system ($\nu = 2$), FM/CAM/SYM phases

[Das Sarma et al, 1998]